CrossMark

RESEARCH PAPER

Pharmaceutical Potential of a Novel Chitosan Derivative Schiff Base with Special Reference to Antibacterial, Anti-Biofilm, Antioxidant, Anti-Inflammatory, Hemocompatibility and Cytotoxic Activities

Sameh S. Ali [1,2] • El-Refaie Kenawy [3] • Fatma I. Sonbol [4] • Jianzhong Sun [1] • Marwa Al-Etewy [3] • Asmaa Ali [5] • Liu Huizi [1] • Nessma A. El-Zawawy [2]

ABSTRACT

Purpose Chitosan and its derivatives possess several unique properties relevant in the field of pharmaceutics and medicinal chemistry. This study aimed to evaluate the pharmaceutical performance of an innovative chitosan derivative, methyl acrylate chitosan bearing *p*-nitrobenzaldehyde (MA*CS*pNBA) Schiff base.

Methods The antibacterial activity of MA*CS*pNBA was tested against multi-drug resistant (MDR) Gram-negative and Gram-positive bacteria using agar-well diffusion method. Anti-biofilm formation was analyzed using a microtitre plate. Antioxidant assays were performed to assess the scavenging activity of MA*CS*pNBA using DPPH, hydrogen peroxide, superoxide together with its reducing power activity. Anti-inflammatory activity was evaluated by albumin denaturation, membrane stabilization, and proteinase inhibition methods.

MA*CS*pNBA was tested for its hemolytic efficiency on human erythrocytes. Cytotoxicity of MA*CS*pNBA was evaluated by MTT assay.

Results MA*CS*pNBA showed a significant performance as an antibacterial candidate against MDR bacteria, anti-biofilm, antioxidant and anti-inflammatory biomaterial, evidencing hemocompatibility and no cytotoxicity. It exhibited a significant negative correlation with biofilm formation by the MDR-PA-09 strain. Biological activities were found to be significantly concentration-dependent.

Conclusions the newly chitosan derivative MA*CS*pNBA showed to be promising for pharmaceutical applications, expanding the treatment ways toward skin burn infections since it allied excellent antibacterial, anti-biofilm, antioxidant, anti-inflammatory, hemocompatibility and absence of cytotoxic activities.

KEY WORDS antibacterial · antioxidant · anti-inflammatory · chitosan Schiff bases · cytotoxicity

✉ Sameh S. Ali
samh_samir@science.tanta.edu.eg; samh@ujs.edu.cn

✉ Jianzhong Sun
jzsun1002@ujs.edu.cn

[1] Biofuels Institute, School of the Environment and Safety Engineering Jiangsu University, Zhenjiang 212013, China

[2] Botany Department, Faculty of Science Tanta University, Tanta 31527, Egypt

[3] Polymer Research Group, Department of Chemistry, Faculty of Science Tanta University, Tanta 31527, Egypt

[4] Department of Microbiology, Faculty of Pharmacy Tanta University, Tanta 31527, Egypt

[5] Ministry of Health and Population, Chest Directorate Abbassia Chest Hospital, Cairo, Egypt

ABBREVIATIONS

BSA	Bovine serum albumin
CrI	Crystallinity index
DMEM	Dulbecco's Modified Eagle's medium
DMSO	Dimethyl sulfoxide
DPPH	2,2-diphenyl-2-picrylhydrazyl
DRPs	Drug resistance profiles
EC_{50}	Effective concentration 50
FT-IR	Fourier transform infrared
H_2O_2	Hydrogen peroxide
IZD	Inhibition zone diameter
MA*CS*pNBA	Aminated chitosan bearing *p*-nitrobenzaldehyde
MCF-10A	Normal breast epithelial cell line
MCF-7	Cancerous breast epithelial cell line

MDR	Multi-drug resistance
MDR-EC	MDR *Escherichia coli*
MDR-KP	MDR *Klebsiella pneumonia*
MDR-PA	MDR *Pseudomonas aeruginosa*
MDR-SA	MDR *Staphylococcus aureus*
MHA	Mueller-Hinton agar
MHB	Mueller-Hinton broth
MIC	Minimum inhibitory concentration
MTT	3-(4,5-dimethylthiazol-2-yl)-2, 5-diphenyltetrazolium bromide
NIH-3 T3	Mouse embryonic fibroblast cell line
PBS	Phosphate buffered saline
RBCs	Red blood cells
RCV	Relative cell viability
TCA	Trichloroacetic acid
TEM	Transmission electron microscope
TGA	Thermogravimetric analysis
TSB	Tryptic Soy Broth

INTRODUCTION

Nosocomial infections by multi-drug resistant (MDR) pathogens remain an intractable challenge in public health management, worldwide (1–3). Of those pathogens, MDR *Pseudomonas aeruginosa* (MDR-PA), MDR *Klebsiella pneumonia* (MDR-KP), MDR *Escherichia coli* (MDR-EC), and MDR *Staphylococcus aureus* (MDR-SA) have been known as most terrible bacterial pathogens of skin burn wound infections (1,4,5), to which novel antimicrobial agents are in demand to cut life-threatening such infections. Therefore, the development of "greener" technologies with fewer side effects against such a catastrophic issue has attracted more and more attention in recent years. The success in designing and development of safe antibacterial candidates, which are distinct from conventional drugs, is the key to combating clinical MDR pathogens.

Chitosan, a natural linear amino-polysaccharide, is one of the most exploited versatile polymers in the pharmaceutical research field. It is a polycationic polymer derived from the shells of crustaceans by partial deacetylation of chitin (6). It has gained wide interest for pharmaceutical applications such as drug delivery, enzyme immobilization, and tissue engineering (7,8) because of its unique properties such as biocompatibility, biodegradability, non-immunogenicity, and non-toxicity (9–11). Despite the advantages above, chitosan exhibits insolubility in water due to the pKa value which is closed to 6.5. It shows poor solubility in the acidic environment since the primary amine of chitosan gets protonated and produces a positively charged polycation (12). Therefore, chemical modifications can enhance the solubility of chitosan, since a number of free amino and hydroxyl groups increases, which can easily form a complex with polyanions without affecting the original cationic properties (13). Schiff bases-based chitosan represents an important class of chemical modifications, formed by the conjugation of a primary amine on chitosan with an active carbonyl group (14). The substitution reaction is very easy to produce imine-containing Schiff bases (15). The relation between chitosan Schiff-bases and their wide range of pharmacological activities has been established previously (12,15,16).

To the best of our knowledge, preparation of an innovative chitosan Schiff base based on aminated chitosan conjugated with *p*-nitrobenzaldehyde has not been reported previously. Therefore, our group has lately developed a newly functionalized chitosan derivative, methyl acrylate chitosan bearing *p*-nitrobenzaldehyde (MA*CS*pNBA) by a Schiff base reaction in three steps as shown in Scheme 1: (i) we carried out a functionalization reaction to obtain methyl acrylate chitosan. This step was carried out in the presence of an excess of methyl acrylate and at room temperature. (ii) methyl acrylate chitosan was further subjected to amination reaction using ethylenediamine to enhance the functionality of the newly synthesized chitosan derivative, and (iii) finally, the aminated chitosan has been equipped with *p*-nitrobenzaldehyde via Schiff base reaction. The functionalization reaction successfully took place at room temperature, avoiding the polymerization of methyl acrylate and instead it reacted entirely with chitosan.

Although chitosan was established previously in various studies as an antimicrobial agent, continuous mutations of bacteria to resist multiple antibiotics have driven scientists to develop an effective antimicrobial agent against clinical MDR bacteria. Therefore, this study was aimed at evaluating the pharmaceutical action of the newly synthesized chitosan derivative, MA*CS*pNBA, with special reference to antibacterial, anti-biofilm, antioxidant, anti-inflammatory effects. Hemocompatibility and cytotoxic activities of the MA*CS*pNBA were also examined to evaluate the performance of this modified Schiff base as a new leading structure in the pharmaceutical field.

MATERIALS AND METHODS

Materials

Azocasein, trichloroacetic acid (TCA), Nitro blue tetrazolium, potassium ferricyanide, ascorbic acid, phosphate buffered saline (PBS), 2,2-diphenyl-2-picrylhydrazyl (DPPH), crystal violet, Dulbecco's Modified Eagle's medium (DMEM), 3-(4,5-dimethylthiazol-2-yl)-2,5-diphenyltetrazolium bromide (MTT), and MTT formazan purple crystals were from Sigma-Aldrich (St. Louis, USA). Bovine serum albumin (BSA) solution was from Merck (Darmstadt, Germany). Aspirin was from Bayer (Leverkusen, Germany) and dimethyl

sulfoxide (DMSO) was from Loba Chemie (Mumbai, India). Mueller-Hinton medium was from Difco (San Diego, USA). NIH-3 T3 (Mouse embryonic fibroblast), MCF-10A (normal breast epithelial), and MCF-7 (cancerous breast epithelial) cell lines were obtained from the American Type Culture Collection (Minnesota, USA).

Bacterial Strains and Culture

Sixteen MDR bacterial strains isolated and identified from skin burn wound infections were chosen from our previous studies (1,5,12), including MDR-PA (6 strains), MDR-KP (5 strains), MDR-SA (4 strains), and one strain of MDR-EC. These strains were strong biofilm-producers. Drug resistance profiles (DRPs) of these strains were presented in **Supplementary Table S1**. Prior to the assays, the strains were cultured in Tryptic Soy Broth (TSB) and incubated at 37°C for 18 h.

Antibacterial Activity

MA*CS*pNBA was evaluated for antibacterial activity against the aforementioned MDR bacteria by agar-well diffusion method as we described previously in detail (1) with a minor modification. Briefly, 100 μL of overnight cultures adjusted to 1×10^7 CFU/mL were spread over Mueller-Hinton agar (MHA) plates. Different concentrations of MA*CS*pNBA (50, 100, 200 and 300 μg/mL) were prepared. In each well, 25 μL of prepared concentrations were loaded and tested against MDR strains. Following which, the inoculated plates were incubated for 18 h at 37°C and inhibition zone diameters (IZDs) were measured (17).

The minimum inhibitory concentration (MIC) of MA*CS*pNBA was determined in accordance with the Clinical and Laboratory Standards Institute (CLSI) guidelines. Serial two-fold dilutions of MA*CS*pNBA were prepared and the opacity was measured using a microtitre plate reader (Infinite F50, Tecan, Switzerland) at 578 nm. The MIC was defined as the lowest concentration of MA*CS*pNBA at which no visible bacterial growth was observed.

The mechanism of antibacterial action of the MA*CS*pNBA was examined by transmission electron microscope (TEM). The morphological changes of MDR-PA-09 and MDR-SA-04 strains treated with MA*CS*pNBA were examined under a JEM-100SX TEM (JEOL, Japan) as we described previously (1,4,5,12).

Anti-Biofilm Activity

Our preliminary experiments to evaluate the qualitative and molecular expression of biofilm-related genes revealed that MDR-PA-09 was the highest biofilm-producing strain (data not shown). The anti-biofilm potential of the MA*CS*pNBA was screened against the MDR-PA-09. The effect of the MA*CS*pNBA on biofilm formation was analyzed using a microtitre plate reader (Infinite F50, Tecan, Switzerland). The bacterial culture was grown in Mueller-Hinton broth (MHB) medium at 37°C for 24 h and then suspended in sterile normal saline solution (0.85% NaCl) to obtain an inoculum equivalent to 1×10^7 CFU/mL. To each well, it was added 80 μL of the adjusted MDR-PA-09 inoculum, 80 μL of the MA*CS*pNBA (100–500 μg/mL) and 40 μL of MHB medium. After incubation at 37°C for 48 h, wells were washed three times with saline solution. The adhered biofilm layer was stained with crystal violet (1% w/v) for 15 min at room
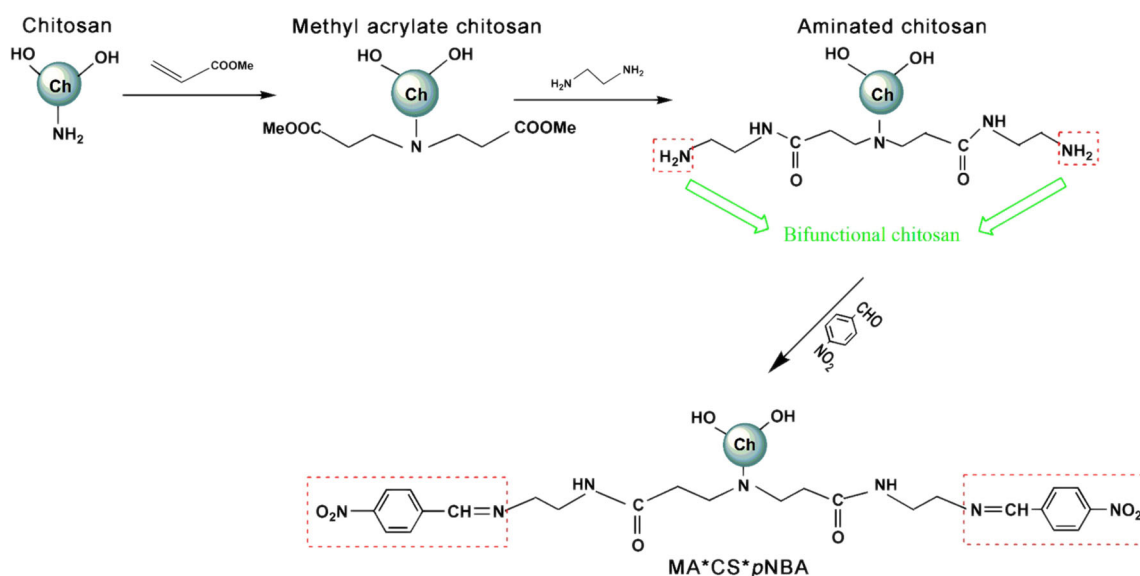
Scheme I Synthetic pathway for the preparation of MA*CS*pNBA Schiff base.

temperature. Next, wells were washed with water and acetic acid to release the stain bound to the biofilm. The absorbance was measured spectrophotometrically at 570 nm.

Antioxidant Activity

The antioxidant activity of MA*CS*pNBA was assessed using four kinds of antioxidant assays, including DPPH assay (3), hydrogen peroxide (H_2O_2) assay (18), superoxide assay (19) and reducing power assay (20). Meanwhile, ascorbic acid was used as positive control. For DPPH radical scavenging assay, DPPH$^.$ was measured at 517 nm using a UV–visible spectrophotometer (Shimadzu-UV2600, Japan). The lower absorbance of the reaction mixture indicates higher free radical scavenging activity. The antioxidant activity by DPPH was calculated using the formula: scavenging effect (%) = 1-(A_T/A_C)*100, where A_T is the absorbance of the tested sample and Ac is the absorbance of the control reaction at 517 nm. Effective concentration 50 (EC_{50}, μg/mL) was defined as the concentration at which 50% of DPPH radicals were scavenged. Estimation of antioxidant activity by H_2O_2 assay was carried spectrophotometrically at 230 nm. The H_2O_2 scavenging activity percentage was calculated using the formula: scavenging effect (%) = 1- (A_T/A_C)*100, where A_T is the absorbance of the tested sample and Ac is the absorbance of the control reaction at 230 nm. EC_{50} was the effective concentration at which 50% H_2O_2 were scavenged. The superoxide scavenging ability of MA*CS*pNBA was read at 560 nm. The capability of scavenging the superoxide radical was calculated using the formula: scavenging effect (%) = 1- (A_T/A_C)*100, where A_T is the absorbance of the tested sample and Ac is the absorbance of the control reaction at 560 nm. EC_{50} was calculated as the effective concentration at which 50% superoxide were scavenged. The reducing power of MA*CS*pNBA was measured at the absorbance of 700 nm. Increased absorbance of the reaction mixture indicates increased reducing power. EC_{50} was the effective concentration at the reducing power absorbance of 0.5.

Anti-Inflammatory Activity

As MA*CS*pNBA showed potential antibacterial, anti-biofilm, and antioxidant performance, this newly synthesized chitosan derivative was employed to evaluate its anti-inflammatory activity by albumin denaturation, membrane stabilization of red blood cells (RBCs) assay, and proteinase inhibition methods as described in details in our earlier study (1). Different concentrations (100, 200, 300, 400, 500, 1000 and 2000 μg/mL) of MA*CS*pNBA were prepared and aspirin has been used as a standard drug. For albumin denaturation assay, the absorbance was measured at 660 nm using a UV–visible spectrophotometer (Shimadzu-UV2600, Japan) and the inhibition of albumin denaturation was calculated using

the formula: inhibition (%) = $[(A_C - A_T)/A_C]$*100, where A_C is the absorbance of control in the absence of aspirin and A_T is the absorbance of tested sample. The anti-inflammatory activity of MA*CS*pNBA was also determined by membrane stabilization assay in the presence of human RBCs. The absorbance was measured at 560 nm and the percent inhibition of hemolysis of the MA*CS*pNBA was calculated using the formula: Inhibition of hemolysis (%) = $[(A_C - A_T)/A_C]$*100, where A_C is the absorbance of control in the absence of aspirin and A_T is the absorbance of the tested sample. Proteinase inhibitory activity against azocasein was detected according to the method reported previously (1). The absorbance was measured at 440 nm and the percent inhibition of proteinase activity was calculated as mentioned above.

Hemolysis Activity

The hemocompatibility test was performed to measure the extent of the destruction of RBCs caused by MA*CS*pNBA when it comes into contact with human erythrocytes as described by Upadhyay et al. (21) with a minor modification. Briefly, MA*CS*pNBA with different concentrations of 0.5, 1.0, and 1.5 mg/mL were dispersed in a phosphate buffered saline (PBS). Triton X-100 and PBS were used as positive and negative controls, respectively. The free hemoglobin concentration as a measure of hemolysis was measured spectrophotometrically at 545 nm. The percentage of hemolysis was calculated using the formula: hemolysis (%) = $[(A_T - A_N)/(A_P - A_N)]$*100, where A_T, A_N and A_P are the absorbance values of the tested sample, negative control, and positive control, respectively.

Cytotoxicity Using MTT Assay

The cytocompatibility of MA*CS*pNBA was investigated by the MTT assay using a series of cell lines, including NIH-3 T3 (Mouse embryonic fibroblast) as fibroblast cells play an important role in wound repair, MCF-7 (luminal A-like breast cancer cells), and MCF-10A (normal breast cells). The viability of NIH-3 T3, MCF-7 and MCF-10A cells in the presence of different concentrations (10, 50, 100, 500 and 1000 ppm) of MA*CS*pNBA were quantified according to the method reported by Liu et al. (22). The optical density at 490 nm was detected using a microplate reader and the relative cell viability (RCV) was calculated using the formula: RCV (%) = (OD_T/OD_C)*100, where OD_T and OD_C are the absorbance values of test and control groups, respectively.

Statistical Analysis

Data were expressed as the mean ± standard deviation (SD) from three replicates. Statistical comparisons were determined by one-way, two-way and three-way analysis of variance

**Table I** Antibacterial Activity of MA*CS*pNBA Schiff Base against 16 MDR Bacterial Strains

| Strain	IZD (mm)				$P^{\#}$
	Concentration of MA*CS*pNBA (μg/mL)				
	50	**100**	**200**	**300**	
Gram-negative bacteria					
MDR-PA-02	11.2 ± 0.09	13.8 ± 0.08	16.2 ± 0.07	18.1 ± 0.09	< 0.001
MDR-PA-06	9.0 ± 0.07	10.2 ± 0.06	13.8 ± 0.06	15.5 ± 0.07	< 0.001
MDR-PA-07	0.0 ± 0.0	8.5 ± 0.07	10.1 ± 0.05	14.6 ± 0.06	< 0.001
MDR-PA-09	10.5 ± 0.03	12.9 ± 0.06	17.7 ± 0.04	22.1 ± 0.05	< 0.001
MDR-PA-10	0.0 ± 0.0	10.0 ± 0.05	12 ± 0.03	16.8 ± 0.04	< 0.001
MDR-PA-11	9.0 ± 0.01	11.3 ± 0.04	15 ± 0.02	18.2 ± 0.03	< 0.001
MDR-KP-01	0.0 ± 0.0	0.0 ± 0.0	9.0 ± 0.01	11.0 ± 0.02	< 0.001
MDR-KP-02	0.0 ± 0.0	0.0 ± 0.0	8.3 ± 0.05	10.3 ± 0.01	< 0.001
MDR-KP-03	9.0 ± 0.07	10.1 ± 0.01	12.0 ± 0.04	15.6 ± 0.05	< 0.001
MDR-KP-04	9.2 ± 0.09	11.6 ± 0.05	15.7 ± 0.03	19.1 ± 0.04	< 0.001
MDR-KP-05	9.0 ± 0.11	10.3 ± 0.04	13.7 ± 0.02	17.0 ± 0.03	< 0.001
MDR-EC-03	0.0 ± 0.0	9.2 ± 0.03	10.3 ± 0.01	12.8 ± 0.03	< 0.001
Gram-positive bacteria					
MDR-SA-01	9.0 ± 0.17	13.2 ± 0.05	15.0 ± 0.02	19.8 ± 0.06	< 0.001
MDR-SA-02	10.0 ± 0.19	14.6 ± 0.04	18.7 ± 0.01	22.4 ± 0.05	< 0.001
MDR-SA-03	10.0 ± 0.21	13.1 ± 0.03	17.1 ± 0.05	25.8 ± 0.04	< 0.001
MDR-SA-04	15.0 ± 0.23	16.8 ± 0.02	20.3 ± 0.04	28.5 ± 0.03	< 0.001
$P^{\#}$	< 0.001	< 0.001	< 0.001	< 0.004	

$^{\#}$ Two-way ANOVA with multiple comparison test, P value < 0.05 is considered significant. **IZD**; inhibition zone diameter, **MDR**; multi-drug resistance, **PA**; *Pseudomonas aeruginosa*, **KP**; *Klebsiella pneumonia*, **EC**; *Escherichia coli*, and **SA**; *Staphylococcus aureus*

(ANOVA) with Tukey's test using Minitab 17.1.0.0 for Windows (Minitab Inc., 2013, Pennsylvania, USA). Pearson's correlation was calculated to assess the relationship between continuous variables. Normality was checked by Shapiro-Wilk test. Statistical significance was defined at P values less than 0.05.
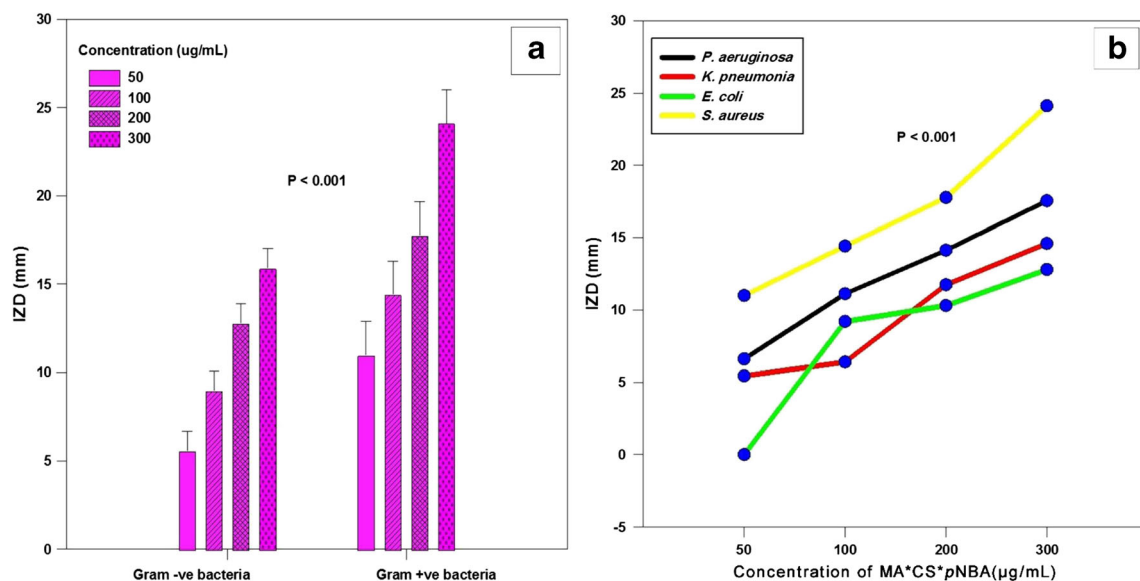
Fig. 1 Effect of different concentrations of MA*CS*pNBA on the inhibition zone diameters (IZDs) of Gram-negative and Gram-positive bacteria (**a**). Effect of different concentrations of MA*CS*pNBA on the IZDs of multi-drug resistant strains *Pseudomonas aeruginosa*, *Klebsiella pneumonia*, *Escherichia coli*, and *Staphylococcus aureus* (**b**). P value < 0.05 is considered significant.
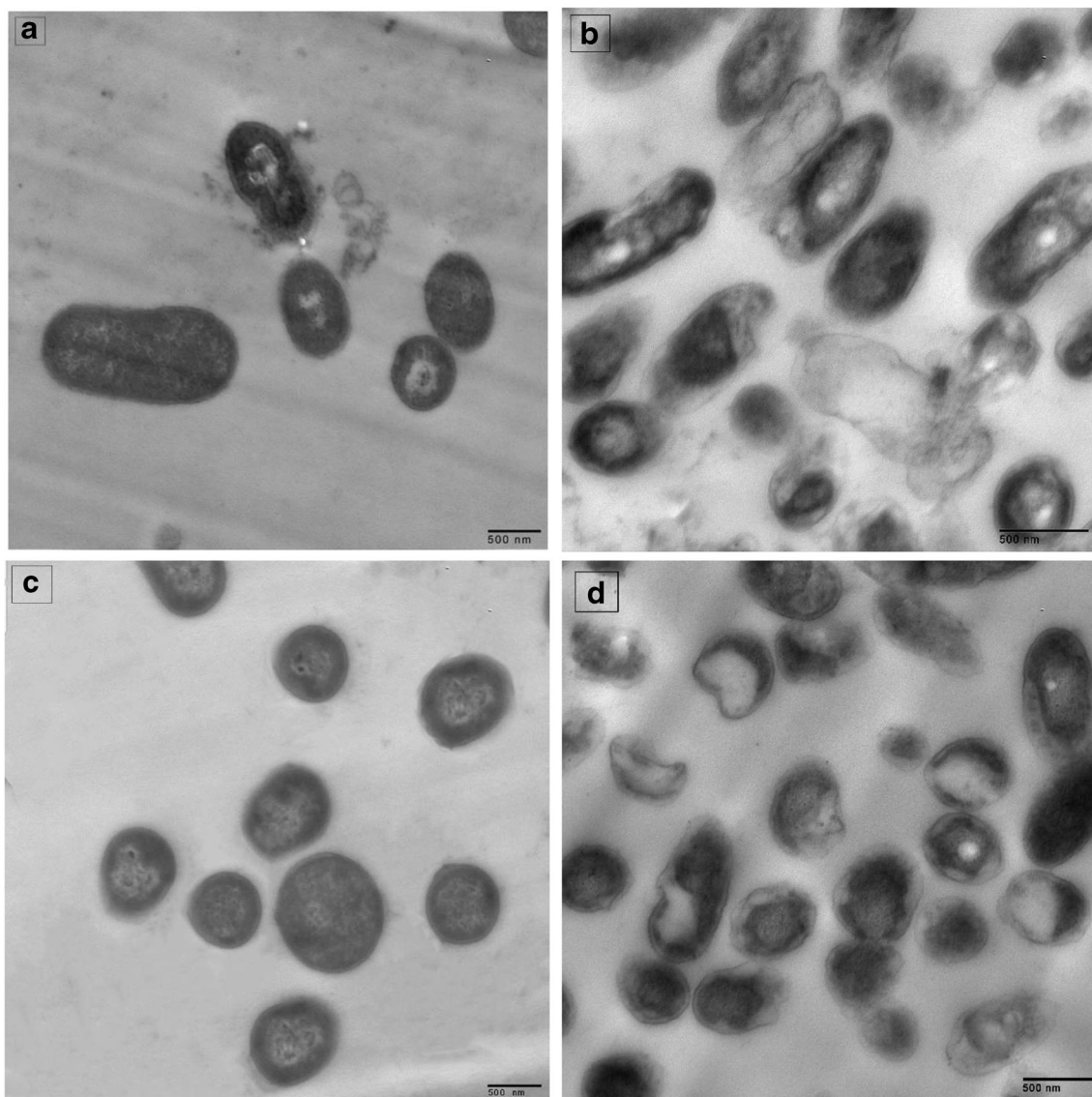
Fig. 2 Transmission electron microscope (TEM) images of MA*CS*pNBA Schiff base–treated MDR-PA-09 and MDR-SA-04 cells (**b** & **d**) against control cells (**a** & **c**), respectively. **MDR**; multi-drug resistance, **PA**, *Pseudomonas aeruginosa*; **SA**, *Staphylococcus aureus*.

RESULTS

Antibacterial Activity of Novel MA*CS*pNBA Schiff Base against MDR Bacteria of Skin Burn Wound Infections

The antibacterial activity of MA*CS*pNBA has been tested *in vitro* against 16 MDR strains of *P. aeruginosa*, *K. pneumonia*, *E. coli*, and *S. aureus*. The modified chitosan Schiff base showed significant inhibitory activity against these bacterial strains. MA*CS*pNBA exhibited distinct differences in the susceptibility in a dose-dependent manner (Table I). The mean IZDs were ranged from zero to 28.5 ± 0.03 mm. Clearly, a comparison of the IZDs among tested Gram-negative and Gram-positive bacterial strains revealed a significant difference between both groups; with a higher antibacterial efficiency against Gram-positive bacteria than that of Gram-negative bacteria ($P < 0.001$) regardless the concentration of the

Table II Anti-biofilm Activity of MA*CS*pNBA Schiff Base against MDR-PA-09 Strain

Concentration (μg/mL)	OD$_{570}$ nm Mean $\pm$ SD
0	0.41 ± 0.05
100	0.25 ± 0.07
200	0.17 ± 0.01
300	0.13 ± 0.04
400	0.09 ± 0.01
500	0.06 ± 0.02
$P^{\#}$	< 0.001

$^{\#}$ One-way ANOVA, P value < 0.05 is considered significant
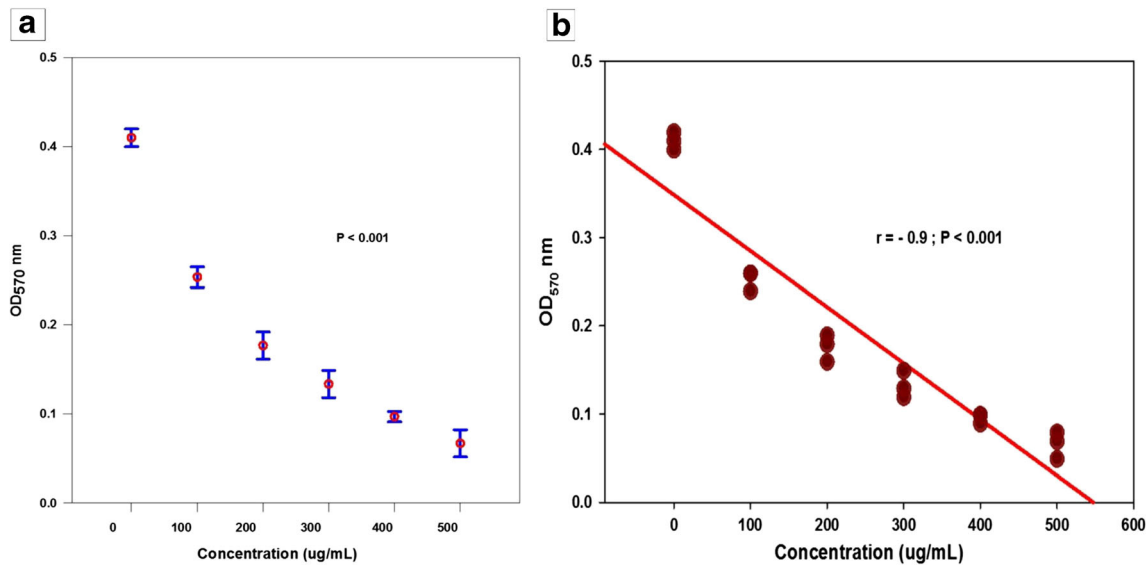
Fig. 3 Anti-biofilm activity against MDR-PA-09 treated with different concentrations of MA*CS*pNBA Schiff base (**a**). Correlation between the concentration of MA*CS*pNBA and biofilm formation (**b**). P value < 0.05 is considered significant.

MA*CS*pNBA (Fig. 1a). The newly synthesized chitosan derivative showed significantly higher antibacterial activity against MDR-SA and MDR-PA compared with other bacteria (P < 0.001) regardless of the concentration of MA*CS*pNBA (Fig. 1b). Additionally, MDR *P. aeruginosa* 9 (MDR-PA-09) and MDR *S. aureus* 4 (MDR-SA-04) strains were found to be more susceptible Gram-negative and Gram-positive bacterial strains to MA*CS*pNBA, respectively and the highest mean IZDs ranged from 10.5 ± 0.03 to 22.1 ± 0.05 mm and from 15.0 ± 0.23 to 28.5 ± 0.03 mm,

Table III   Antioxidant Activity of MA*CS*pNBA Schiff Base Using DPPH, H_2O_2, and Superoxide Radical Assays

Concentration (μg/mL)		Scavenging effect (%)			P^a	P^b
		DPPH	H_2O_2	Superoxide radical		
100	Ascorbic acid	28.8 ± 0.2	29 ± 0.3	96.7 ± 0.3	< 0.001	< 0.001
	Chitosan	7.8 ± 0.4	9.4 ± 0.4	2.8 ± 0.2	< 0.001	
	MA*CS*pNBA	16.8 ± 0.4	14.5 ± 0.4	24.9 ± 0.1	< 0.001	
200	Ascorbic acid	38.7 ± 0.3	39.8 ± 0.3	100 ± 0.0	< 0.001	< 0.001
	Chitosan	22.1 ± 0.3	19.7 ± 0.1	7.9 ± 0.1	< 0.001	
	MA*CS*pNBA	27.4 ± 0.6	25.1 ± 0.3	33.2 ± 0.8	< 0.001	
300	Ascorbic acid	49 ± 0.5	50.3 ± 0.5	100 ± 0.0	< 0.001	< 0.001
	Chitosan	37.5 ± 0.5	32.5 ± 0.5	13.8 ± 0.2	< 0.001	
	MA*CS*pNBA	44.7 ± 0.5	41 ± 0.09	47 ± 0.5	< 0.001	
400	Ascorbic acid	64.7 ± 0.4	65.2 ± 0.4	100 ± 0.0	< 0.001	< 0.001
	Chitosan	52.8 ± 0.4	49.8 ± 0.1	15.7 ± 0.3	< 0.001	
	MA*CS*pNBA	60.2 ± 0.1	58.6 ± 0.4	62.5 ± 0.5	< 0.001	
500	Ascorbic acid	79.1 ± 0.3	78.6 ± 0.3	100 ± 0.0	< 0.001	< 0.001
	Chitosan	66.6 ± 0.3	58.6 ± 0.07	15.7 ± 0.3	< 0.001	
	MA*CS*pNBA	74.8 ± 0.2	70.1 ± 0.3	81.1 ± 0.9	< 0.001	
	P^c	< 0.001	< 0.001	< 0.001		
P^d		< 0.001	< 0.001	< 0.001		

* Three-way ANOVA with multiple comparison test (Tukey's test), P value < 0.05 is considered significant
[a] Comparison of antioxidant methods on the level of tested material
[b] Comparison of antioxidant methods on the level of concentration
[c] Comparison of tested materials on the level of scavenging activity
[d] Comparison of concentrations on the level of scavenging activity

Springer

Table IV Antioxidant Activity of MA*CS*pNBA Schiff Base Using Reducing Power Assay

Concentration (μg/mL)	Reducing power (A)			$P^{\#}$
	Ascorbic acid	**Chitosan**	MA*CS*pNBA	
100	1.2 ± 0.08	0.09 ± 0.01	0.2 ± 0.01	< 0.001
200	2.3 ± 0.1	0.27 ± 0.09	0.77 ± 0.09	< 0.001
300	2.7 ± 0.1	0.34 ± 0.1	0.92 ± 0.1	< 0.001
400	3.1 ± 0.3	0.41 ± 0.09	1.1 ± 0.09	< 0.001
500	3.5 ± 0.09	0.46 ± 0.08	1.3 ± 0.08	< 0.001
$P^{\#}$	0.03	0.03	0.03	

$^{\#}$ Two- way ANOVA with multiple comparison test, P value < 0.05 is considered significant

respectively (Table I). On the other hand, MA*CS*pNBA has the maximum antibacterial activity with a MIC value of 6.25 µg/mL for both bacterial strains.

The modifications in the structure of MA*CS*pNBA Schiff base, as characterized by Fourier transform infrared (FT-IR) spectroscopy, elemental analysis, thermogravimetric analysis (TGA), and XRD spectra (data not shown), are thought to elucidate the possible mechanisms of antibacterial action of MA*CS*pNBA. These postulates depend on the mean IZDs of MA*CS*pNBA against bacteria (Table I) which might be due to the introduction of amino and aldehyde groups onto the chitosan, binding of this novel derivative with the bacterial cell wall, leakage out of intracellular constituents and ultimately cell death would occur.

Based on the aforementioned mechanisms of MA*CS*pNBA antibacterial action, the morphological changes of MDR-PA-09 and MDR-SA-04 strains were examined by a TEM (Fig. 2). The control cells showed intact and clearly discernible cell envelopes with a dense cytoplasmic homogeneity (Fig. 2a, c). In MA*CS*pNBA treated MDR-PA-09 and MDR-SA-04, cells showed deformation and disruption of cell walls or membranes, protruding of the cell envelope, partial to complete loss of cytoplasm, osmotic cell lysis and leakage of intracellular constituents compared with untreated cells (Fig. 2b, d). The overall results suggest that the incorporation of p-nitrobenzaldehyde into aminated chitosan seems to favor the antibacterial activity and it may be a promising potential candidate for pharmaceutical application fields.

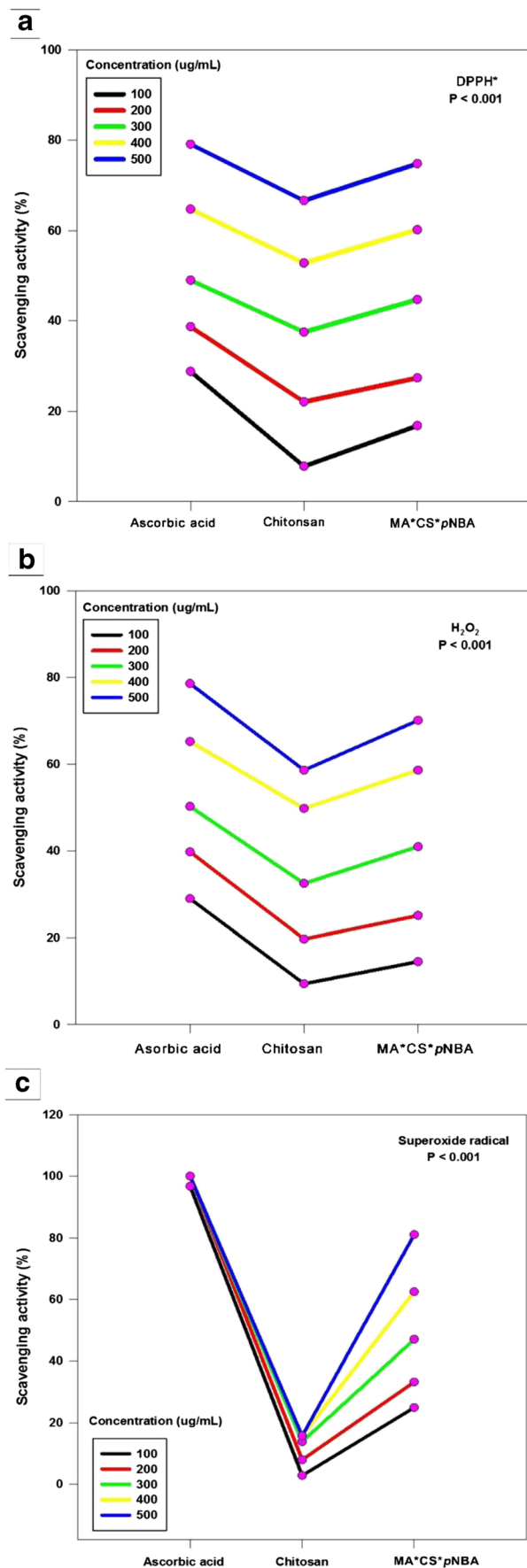## Anti-Biofilm Activity of MA*CS*pNBA on Biofilm-Producing MDR-PA-09 Strain

Here, MA*CS*pNBA has been proven to have antibacterial activity. Therefore, this newly synthesized chitosan derivative has attracted a great attention to evaluating its anti-biofilm activity. MA*CS*pNBA exhibited anti-biofilm activity against MDR-PA-09 strain by inhibiting the biofilm formation (Table II). The percentage of biofilm inhibition was significantly increased ($P < 0.001$) regardless of the MA*CS*pNBA concentration as compared to the corresponding control. The

biofilm formation by MDR-PA-09 was reduced significantly with the increase of MA*CS*pNBA concentration ($P < 0.001$) (Fig. 3a). It was found that, a significant negative correlation ($r = -0.9$; $P < 0.001$) was obtained between the chitosan derivative concentration and biofilm formation by the MDR-PA-09 strain (Fig. 3b).

Antioxidant Activity of MA*CS*pNBA

Antioxidant activities of MA*CS*pNBA were determined by four assays, including DPPH, H_2O_2, superoxide, and reducing power as displayed in Tables III & IV and Figs. 4, 5, 6 and 7. Clearly, the antioxidant activity of MA*CS*pNBA was a concentration-dependent. The DPPH$^{\bullet}$ scavenging assay is one of the most economical methods to measure antioxidant activity. This assay was based on the conversion of DPPH to DPPHH, which results in attenuation of the absorbance value at 517 nm. Obviously, with the increase of the concentration from 100 to 500 µg/mL, the scavenging activities of MA*CS*pNBA, original chitosan, and ascorbic acid were enhanced significantly (Table III). Clearly, the scavenging activity of MA*CS*pNBA was found to be significantly lower than ascorbic acid but higher than that of the chitosan ($P < 0.001$) (Fig. 4a) and the EC_{50} value was found to be 7.8 µg/mL. As depicted in Table III, the H_2O_2 and superoxide radical scavenging activities were significantly increased with the increase of concentrations (100 to 500 µg/mL) of all samples. The EC_{50} values of MA*CS*pNBA were found to be 77.8 µg/mL and 150 µg/mL for H_2O_2 and superoxide radical scavenging activities, respectively. In addition, the H_2O_2 scavenging activity of MA*CS*pNBA was found to be significantly higher than that of the original chitosan ($P < 0.001$) (Fig. 4b). The MA*CS*pNBA had potent superoxide radical scavenging activity although it was lower than ascorbic acid at all tested concentrations ($P < 0.001$) (Fig. 4c). Regardless the type of tested material or the method used to assess the antioxidant activity, a significant positive correlation ($r = 0.5$; $P < 0.001$) was recorded between scavenging activity percentage and the concentration tested (Fig. 5a, b). On the other hand, the antioxidant activity measured by superoxide radical was

significantly higher than that of DPPH and H_2O_2 ($P < 0.001$) (Fig. 6I) and it was significantly increased with the increase of the concentration ($P < 0.001$) (Fig. 6II). Interestingly, the antioxidant activity of MA*CS*pNBA was significantly higher than that of chitosan and more near to ascorbic acid ($P < 0.001$) (Fig. 6III).

The antioxidant activity was also evaluated using reducing power assay. The absorbance of MA*CS*pNBA, chitosan, and ascorbic acid was significantly increased with the increase of the concentration from 100 to 500 µg/mL (Table IV). The EC_{50} value was found to be 112.4 µg/mL. In comparison with ascorbic acid, the reducing power of MA*CS*pNBA remained low. Irrespective of this, the antioxidant activities of MA*CS*pNBA, chitosan, and ascorbic acid were found to be significantly concentration-dependent ($P = 0.03$) (Fig. 7I). At all tested concentrations, the reducing power of ascorbic acid was significantly higher than that of MA*CS*pNBA and chitosan ($P < 0.001$) (Fig. 7II).

Anti-Inflammatory Activity of MA*CS*pNBA

The MA*CS*pNBA was employed to explore its anti-inflammatory activity. The inhibitory activity of MA*CS*pNBA was assessed at various concentrations using albumin denaturation, membrane stabilization, and protein-ase inhibitory activity compared with commercially available aspirin. The results of albumin denaturation indicated a significant increase in inhibiting bovine serum albumin by increasing the concentration of MA*CS*pNBA and a standard drug (aspirin) in a concentration-dependent manner (Table V). The results proved that the MA*CS*pNBA was about the equal percentage of inhibition when compared to the aspirin and they exerted inhibition of 88.9 ± 0.08 and $90.1 \pm 0.15\%$, respectively at 2000 µg/mL. Statistically, a significant difference between the inhibition of albumin denaturation percentage by MA*CS*pNBA and aspirin ($P < 0.001$) has been recorded at all concentrations tested (Fig. 8a).

The MA*CS*pNBA exhibited membrane stabilization of 26.5 ± 0.02 and $91.2 \pm 0.07\%$ for human RBCs as minimum and maximum percentage activities, respectively. The membrane stabilization percentages of MA*CS*pNBA and aspirin were highly similar and they exerted a stabilization of 91.2 ± 0.07 and $91.5 \pm 0.1\%$, respectively at 2000 µg/mL (Table V). Statistically, a significant difference between the percentage of membrane stabilization by MA*CS*pNBA and aspirin has been recorded at any of their concentrations ($P < 0.001$) (Fig. 8b).

Fig. 5 Correlation between scavenging activity percentage of MA*CS*pNBA, chitosan, and ascorbic acid (**a**) and of DPPH, H₂O₂, and superoxide radical assays (**b**) at different concentrations. P value < 0.05 is considered significant.
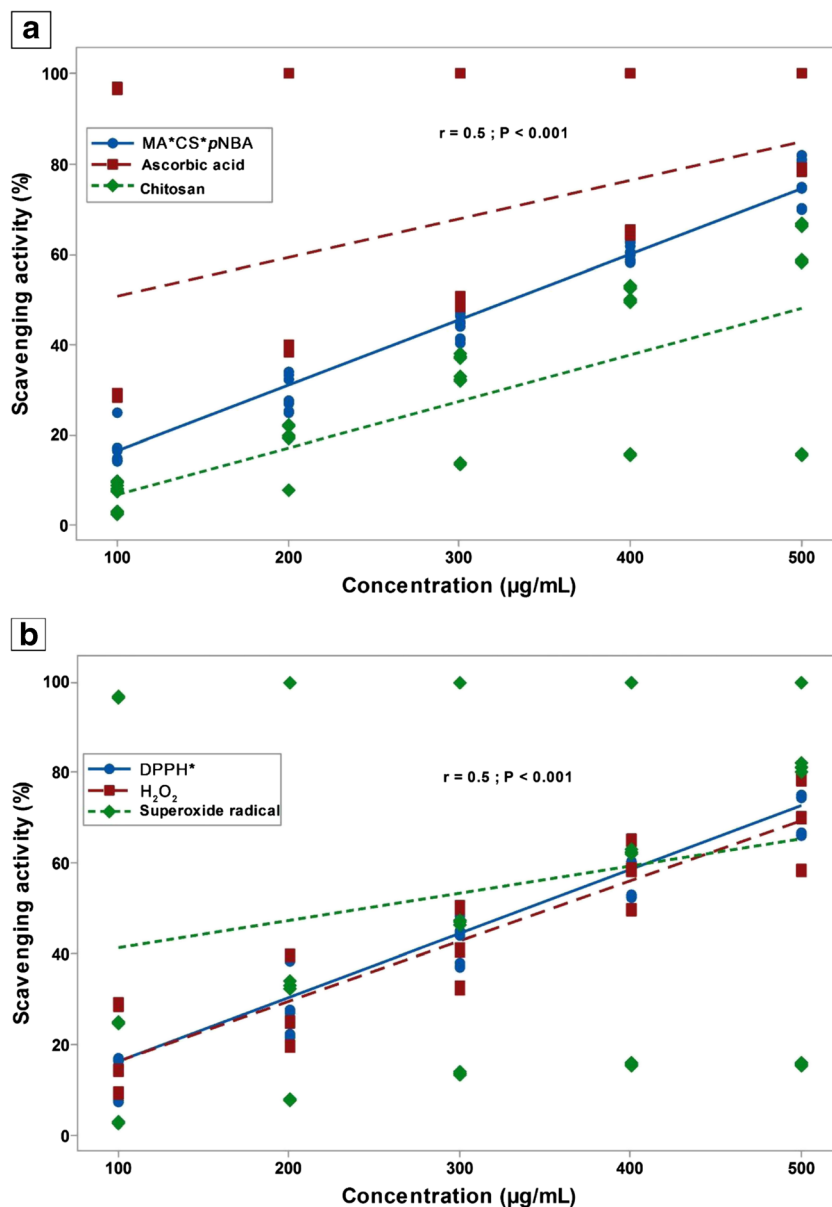
The anti-inflammatory performance of MA*CS*pNBA was also assessed by proteinase inhibition assay and it exhibited a significant activity (Table V). MA*CS*pNBA was similar to aspirin in the inhibition of proteinase and both of them exerted a maximum inhibition of $90.3 \pm 0.07\%$ at $2000 \ \mu g/mL$. Similarly, a significant difference between the inhibitory percentage of proteinase activity by MA*CS*pNBA and aspirin has been recorded at all concentrations tested ($P < 0.001$) (Fig. 8c).

Hemocompatibility Assay

As depicted in Fig. 9, the hemolytic activity of MA*CS*pNBA was clearly concentration-dependent. MA*CS*pNBA exhibited a significant decrease in hemolysis percentage when its

concentration decreased from 1.5 mg/mL to 0.5 mg/mL comparing to Triton X-100 which showed a hemolytic activity of 100% ($P < 0.001$). The hemolytic potential of MA*CS*pNBA was less than 2% suggesting that this novel chitosan derivative met the international standard of biomaterial far less than 5%.

Cytocompatibility Study

To evaluate the biological safety of a material for pharmaceutical applications, cytotoxicity of MA*CS*pNBA was tested on three different cell lines; NIH-3 T3, MCF-7, and MCF-10A of fibroblast wound repair cells, breast cancer cells, and normal breast cells, respectively. The results demonstrated that the MA*CS*pNBA was highly biocompatible (non-cytotoxic),

Fig. 6 Mean of scavenging activity percentage depending on antioxidant activity assays (**I**), tested concentrations (**II**), and tested materials (**III**). P value < 0.05 is considered significant.
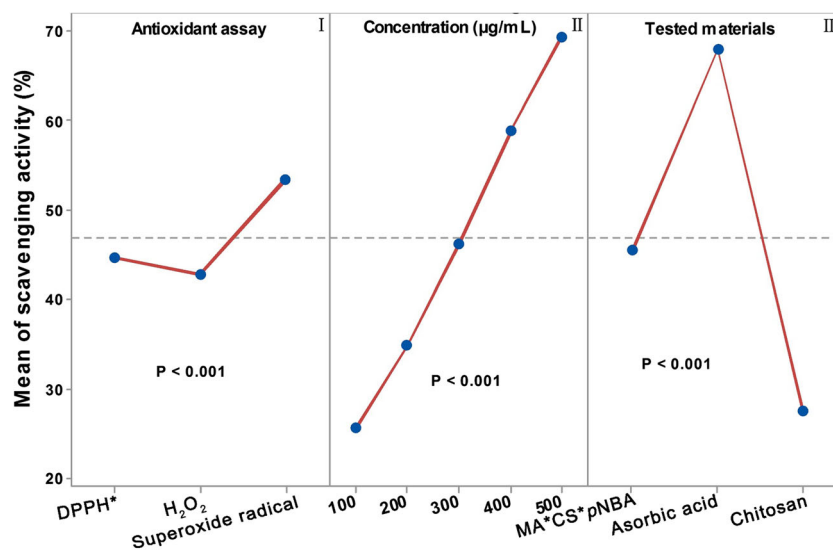
the RCV of MA*CS*pNBA was more than 77%. The RCVs of NIH-3 T3, MCF-7, and MCF-10A cultured with MA*CS*pNBA were more than 92% at the concentration of 50 ppm (Table VI). Clearly, the RCV of MA*CS*pNBA was found to be concentration-dependent; it was decreased with the concentration increased. A statistically significant difference in the mean values between MA*CS*pNBA and chitosan was recorded ($P < 0.001$). This difference was larger than would be expected by chance, taking into account the type of cell line and concentration of tested materials (Table VI). In order to differentiate between groups, a multiple comparison analysis was performed; the effect of different cell line types was found to depend on the existing concentration of tested materials ($P < 0.001$). No significant correlation between the type of cell line and the type of tested material ($P > 0.05$) was observed. Similarly, no

significant correlation between the tested material type and its concentration was observed ($P > 0.05$) (Table VI). On the other hand, the percentage of RCV was significantly depended on the type of cell line tested at concentrations of 100, 500 and 1000 ppm ($P < 0.001$) (Fig. 10a ,b). As presented in Fig. 10c, the cytocompatibility of chitosan in comparison with MA*CS*pNBA was significantly low ($P < 0.001$) (Fig. 11I). In addition, the toxicity of the tested material was significantly increased with the increase of the concentration ($P < 0.001$) (Fig. 11II). Interestingly, the cell viability on NIH-3 T3 was significantly higher compared with other cell lines; MCF-10A and MCF-7 ($P < 0.001$) (Fig. 11III). Regardless of the tested material or the cell line type, a significant negative correlation between the percentage of RCV and the material concentration ($r = -0.8$; $P < 0.001$) was observed (Fig. 12).

Fig. 7 Mean of reducing power depending on tested concentrations (**I**) and tested materials (**II**). P value < 0.05 is considered significant.
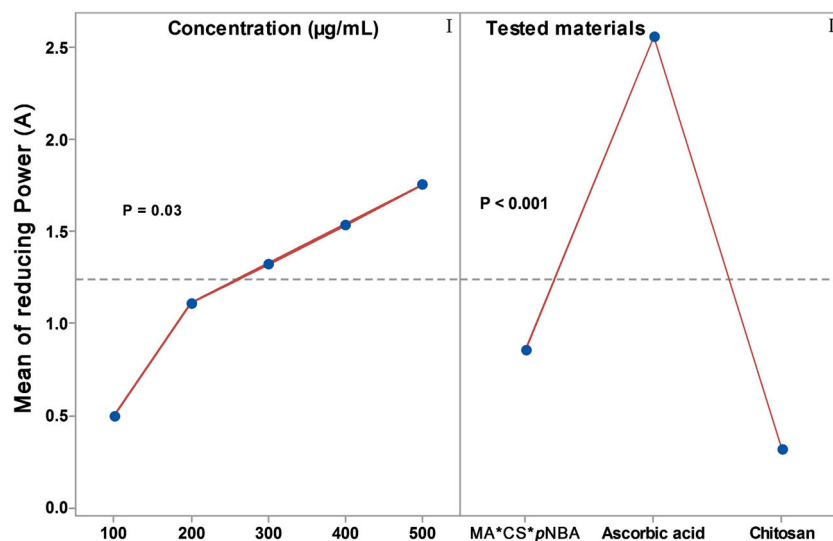
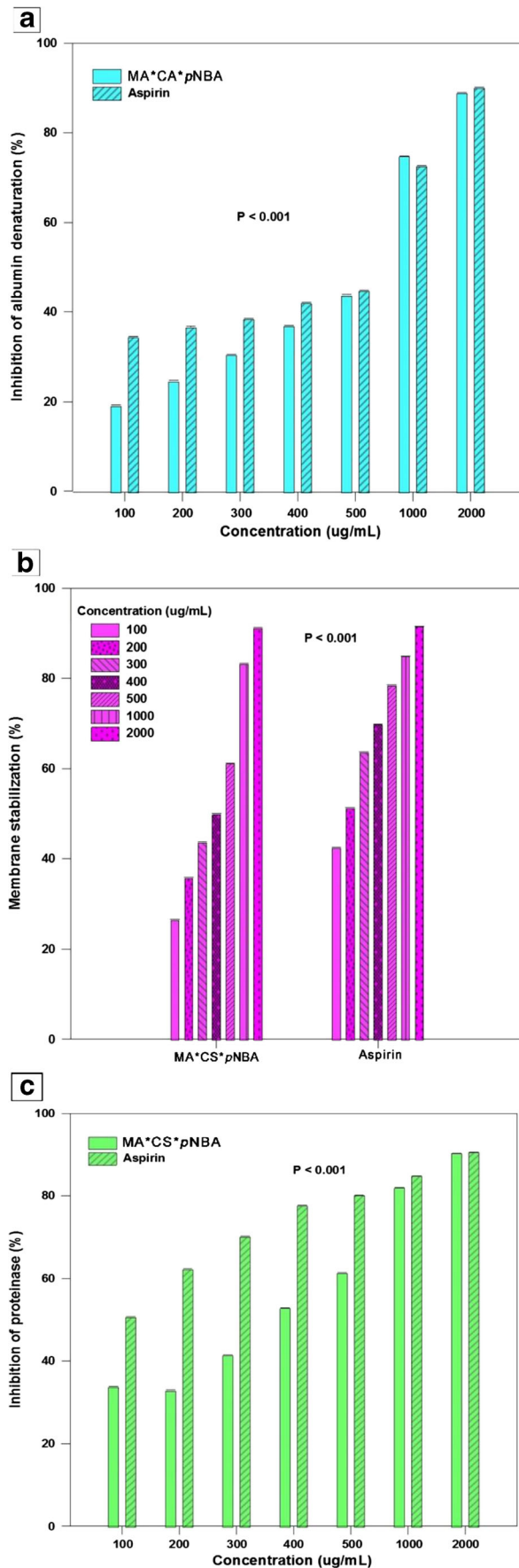**Table V** Anti-inflammatory Activity of MA*CS*pNBA Schiff Base

Assay		Concentration (μg/mL) Anti-inflammatory activity (%)							P#
		100	200	300	400	500	1000	2000	
Inhibition of albumin denaturation	MA*CS*pNBA	19.2 ± 0.02	24.7 ± 0.03	30.5 ± 0.04	36.9 ± 0.05	43.8 ± 0.06	74.8 ± 0.07	88.9 ± 0.08	< 0.001
	Aspirin	34.5 ± 0.09	36.7 ± 0.1	38.5 ± 0.11	42.1 ± 0.12	44.8 ± 0.13	72.6 ± 0.14	90.1 ± 0.15	< 0.001
	P#	< 0.001	< 0.001	< 0.001	< 0.001	< 0.001	< 0.001	< 0.001	
Membrane stabilization	MA*CS*pNBA	26.5 ± 0.02	35.8 ± 0.03	43.8 ± 0.04	50 ± 0.05	61.2 ± 0.06	83.3 ± 0.07	91.2 ± 0.07	< 0.001
	Aspirin	42.6 ± 0.04	51.4 ± 0.05	63.7 ± 0.06	69.9 ± 0.07	78.5 ± 0.08	85 ± 0.09	91.5 ± 0.1	< 0.001
	P#	< 0.001	< 0.001	< 0.001	< 0.001	< 0.001	< 0.001	< 0.001	
Inhibition of proteinase	MA*CS*pNBA	33.9 ± 0.01	33 ± 0.02	41.5 ± 0.03	52.9 ± 0.04	61.4 ± 0.05	82 ± 0.06	90.3 ± 0.07	< 0.001
	Aspirin	50.7 ± 0.02	62.3 ± 0.03	70.2 ± 0.04	77.7 ± 0.05	80.2 ± 0.06	84.8 ± 0.07	90.6 ± 0.08	< 0.001
	P#	< 0.001	< 0.001	< 0.001	< 0.001	< 0.001	< 0.001	< 0.001	

Two- way ANOVA with multiple comparison test, P value < 0.05 is considered significant

DISCUSSION

The emergence of MDR Gram-negative/Gram-positive bacteria is of great worldwide clinical problem. The extensive and misuse of first-line antibiotics to control human infections, such as skin burn, urinary tract, meningitis, and gastroenteritis infections imposed the development of multiple mechanisms of bacterial resistance because of the selective pressure that favors MDR strains mainly in hospital environments. Despite the fact that numerous advanced strategies enable the molecular design of novel drugs for combating and overcoming the antibacterial resistance, the MDR-associated bacterial infections remain a major challenge to modern pharmaceutics and medicinal chemistry. Consequently, this scenario stimulates an urgent need to find new antibacterial agents as alternatives for combating bacterial resistance [23]. It is noteworthy that the antibacterial activity of MA*CS*pNBA Schiff base had the potential to inhibit the growth of Gram-positive bacteria over Gram-negative bacteria as confirmed by the mean IZDs due to the difference in cell wall structure [3–5]. Clearly, the newly synthesized chitosan derivative MA*CS*pNBA showed a good capability in inhibiting the MDR bacterial pathogens of skin burn infection, which could effectively result in the improved wound healing ability [12,24]. In this context, a newly synthesized chitosan derivative, hydroxyapatite-chitosan, has been reported as a potential sunscreen gel against MDR-PA, MDR-KP, and MDR-SA bacteria of skin burn infections and it was a promising antibacterial chitosan derivative agent for skin health care as reported in our earlier study [12].

The potential disruptive action of MA*CS*pNBA on the MDR bacteria was probably based on the structure of this modified derivative. The results of FT-IR, XRD, TGA, and elemental analysis demonstrated that the MA*CS*pNBA was successfully synthesized via Schiff base reaction and explained the possible mechanisms of its antibacterial action. FT-IR spectroscopy revealed that the presence of -N=CH- besides the stretching vibration of C=C and C-H bonds, belonging to the aromatic rings of the aldehyde, are thought to be important factors contributing the antibacterial activity of MA*CS*pNBA Schiff base. The XRD diffractogram of MA*CS*pNBA showed a characteristic peak at $2\theta = 20.4°$ and $12.2°$, suggesting the increased possibility for hydrogen bond formation after Schiff base reaction. The crystallinity index (CrI) value of MA*CS*pNBA (39.0%) was found to be lower than that of the original chitosan, which might be due to the hydrogen bond deformation and a substitution of the p-nitrobenzaldehyde on the nitrogen atoms. The decrease in CrI value may be the reason for potential antibacterial activity by attaching of MA*CS*pNBA to the bacterial cell membrane through the functional $-NH_2$ and p-nitrobenzaldehyde groups. On the other hand, the C/N ratio of MA*CS*pNBA was obviously lower than that of the original chitosan, indicating

the introduction of the p-nitrobenzaldehyde on the modified aminated chitosan, which attributed to the disruption of bacterial cell membranes followed by a biocidal activity. The TGA analysis of MA*CS*pNBA revealed a higher thermal stability compared to that of chitosan, which might be related to the substitution effect of the NO_2 moiety. Hence, MA*CS*pNBA exhibited broad-spectrum antibacterial activity. The relation between the polycationic nature of chitosan and its antibacterial activity has been established in several reports (12,25,26). The electrostatic interaction between the positively charged -NH_2 groups of the MA*CS*pNBA and the negatively charged bacterial cell surface may the binding of modified chitosan with bacterial nucleic acid, compromise membrane permeability, interfere with the synthesis of membrane proteins thereby affecting structure and function of the bacterial cell (12). The newly synthesized chitosan derivative may serve as a new leading structure for the future design of antibacterial agents.

The wound infections caused by biofilm-producing bacteria, including MDR-PA represent a challenge to clinical diagnosis and failure of treatment that generate strong resistance mechanisms to antibacterial therapy (1). To date, no antibiotic has been developed against biofilm-producing bacteria due to inherent resistance to conventional antibiotics (27). In recent studies, chitosan has well-recognized as an antibacterial agent that showed promising activity to combat or reduce biofilm-associated infections (28,29). MA*CS*pNBA could make the bacterial cell membrane of MDR-PA-09 weakened or even broken. The polycationic nature of MA*CS*pNBA with high surface charge may interact more effectively with the bacterial biofilm layer, and therefore it has a high affinity to bind to bacterial cells. Additionally, the modified chitosan derivative containing a large number of -NH_2 and p-nitrobenzaldehyde groups could contribute to a large surface area and cause MA*CS*pNBA to be adsorbed more tightly on the surface of MDR-PA-09 cells and thus disrupt the bacterial membrane integrity. Collectively, the MA*CS*pNBA was a potential anti-biofilm candidate against the highest biofilm-producing strain, MDR-PA-09. To the best of our knowledge, this study might be the first to evaluate the activity of MA*CS*pNBA against MDR pathogens and biofilm formation, and thus opening a new window for further research and development on this newly synthesized chitosan derivative for its translation into therapeutic strategies.

Antioxidants in a moderate concentration can significantly improve skin burn wound healing (30). Here, antioxidant activities of MA*CS*pNBA were determined by four assays, including DPPH, H_2O_2, superoxide, and reducing power. It has been reported that the antioxidant activity of natural

Fig. 9 Haemocompatibility of MA*CS*pNBA Schiff base. Triton X-100 and phosphate buffered saline (PBS) are positive and negative controls, respectively. P value < 0.05 is considered significant.
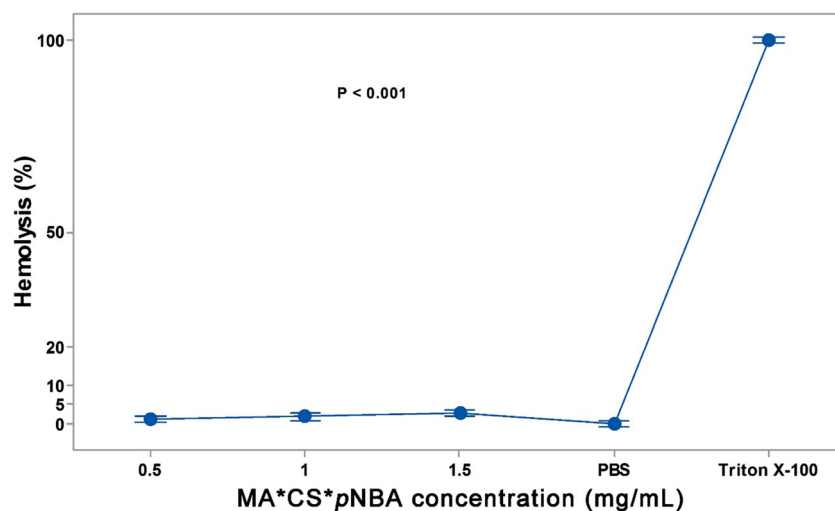
products can confer amazing mechanical protection against oxidative stress-related disorders (31). The EC_{50} value for MA*CS*pNBA was 7.8 µg/mL indicating that though the antioxidant activity of MA*CS*pNBA was lower than ascorbic acid, it had potent DPPH$^{\bullet}$ scavenging activity, which might be due to the nitrogen in this newly modified chitosan derivative (32). The results obtained from the scavenging activity of H_2O_2 and superoxide radical suggest that the enhanced scavenging potential by MA*CS*pNBA might be due to the introduction of p-nitrobenzaldehyde, which could enhance its biological activity. On the other hand, it has been reported that the damaging effect of H_2O_2 in the human body was similar to that of the free radicals. It could react with superoxide anion radical and Fe^{2+} to

form hydroxyl radical (33). Clearly, the antioxidant potential assessed by the aforementioned methods proved that MA*CS*pNBA possessed a higher percentage of scavenging potential which capacitates it exquisite modified chitosan candidate for wound healing.

The antioxidant activity of MA*CS*pNBA was also evaluated using reducing power assay as an important indicator of compounds. In this assay, the antioxidant reacts with Fe^{3+} complex ferricyanide to form the ferrous form. The resulting potassium ferrocyanide, $K_4Fe^{2+}(CN)_6$, could further react with ferric chloride to form Prussian blue $(Fe_4[Fe(CN)_6]_3)$. Therefore, the reducing power could be monitored by the increase in the density of the Prussian blue color in the reaction medium at 700 nm. To the best of the authors'

Table VI   Cytotoxic Activity of MA*CS*pNBA Schiff Base on Three Different Cell Lines; NIH-3 T3, MCF-10A, and MCF-7

Concentration (ppm)		Relative cell viability (%)			P^a	P^b
		NIH-3 T3	**MCF-10A**	**MCF-7**		
10	Chitosan	98.8 ± 1.1	99 ± 1.3	97.1 ± 1.2	> 0.05	> 0.05
	MA*CS*pNBA	97.1 ± 1.5	96.2 ± 1.1	95.3 ± 0.09	> 0.05	
50	Chitosan	96 ± 1.4	95.4 ± 1.3	93 ± 1.1	> 0.05	> 0.05
	MA*CS*pNBA	94.4 ± 1.4	93.7 ± 1.5	92.4 ± 1.4	> 0.05	
100	Chitosan	94.5 ± 1.3	91.1 ± 1.4	90.3 ± 1.3	> 0.05	< 0.05
	MA*CS*pNBA	92.3 ± 1.6	89.3 ± 1.3	86.2 ± 1.6	< 0.05	
500	Chitosan	91.6 ± 1.8	87.5 ± 1.8	82.5 ± 1.3	< 0.001	< 0.001
	MA*CS*pNBA	89.3 ± 1.4	84.6 ± 1.8	81.6 ± 1.2	< 0.001	
1000	Chitosan	88.1 ± 2	82.3 ± 1.3	80.1 ± 1.5	< 0.001	< 0.001
	MA*CS*pNBA	84.7 ± 1.7	79.4 ± 1.7	77.3 ± 1.0	< 0.001	
	P^c	< 0.001	< 0.001	< 0.001		
P^d		< 0.001	< 0.001	< 0.001		

* Three-way ANOVA with multiple comparison test (Tukey's test), P value < 0.05 is considered significant

[a] Comparison of cell line types on the level of tested material

[b] Comparison of cell line types on the level of concentration

[c] Comparison of tested materials on the level of cell line type

[d] Comparison of concentrations on the level of cell line type
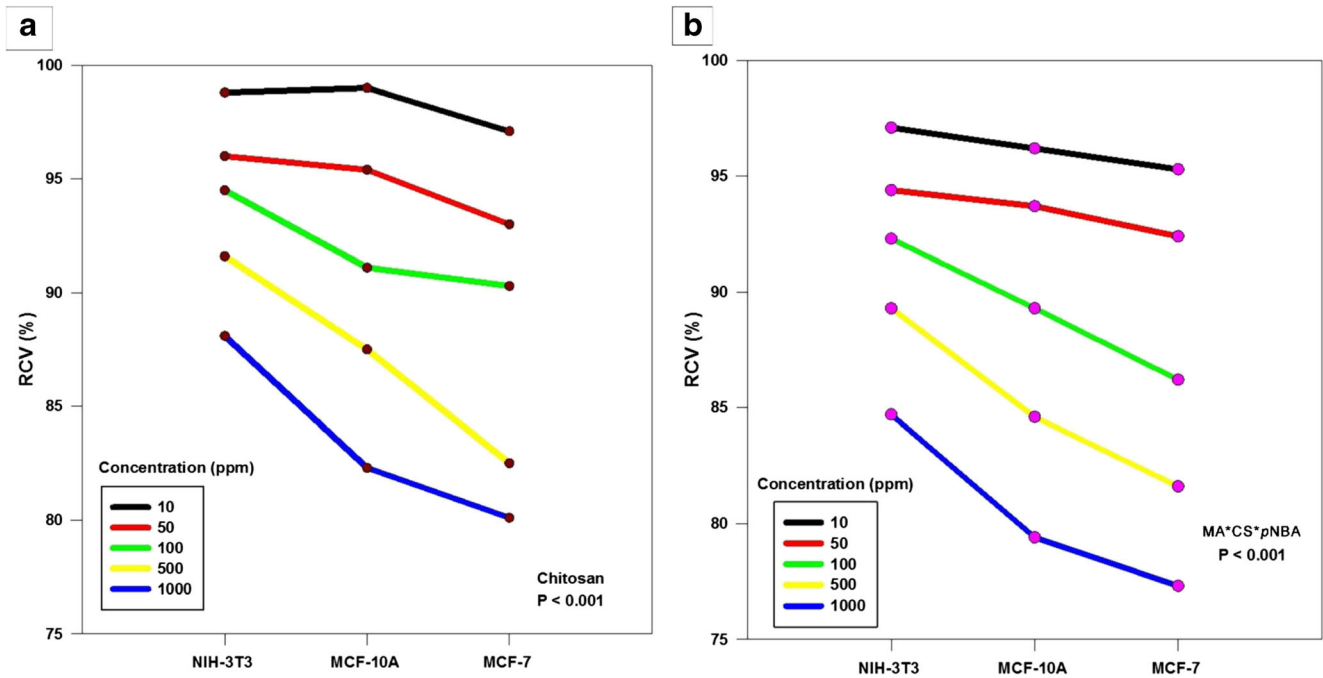
Fig. 10 Cytotoxic activity of MA*CS*pNBA Schiff base. Three-way ANOVA of cell line type and different concentrations of chitosan (**a**) or MA*CS*pNBA (**b**) on the cell viability. **RCV**; relative cell viability, P value < 0.05 is considered significant.

knowledge, the antioxidant activity of MA*CS*pNBA Schiff base has never been investigated before. The data explained that the introduction of the p-nitrobenzaldehyde to the aminated chitosan showed a considerable increase in the amount of scavenging activity and reducing power of the newly synthesized chitosan derivative than the original chitosan. Hence, the results of MA*CS*pNBA may pave the way to confirm the mechanism of action of this novel candidate that can be applied in pharmaceutical applications. As far as we know, there are very few reports focused on the antioxidant activity of modified chitosan derivatives synthesized by chemical modification (18,19).

To explore the anti-inflammatory activity of MA*CS*pNBA, albumin denaturation, membrane stabilization, and proteinase inhibitory were assessed. Membrane stabilization is a biological process of maintaining the integrity of cellular membranes such as RBCs and lysosome against lytic inducers of heat and osmosis (34). The oxidative damage of the erythrocyte membrane was the most obvious reason for the attenuated capacity of RBCs to withstand osmotic and mechanical stresses (35). Our findings of albumin denaturation were found in agreement with the reports of Ali *et al.* (1) and Govindappa *et al.* (36). Recently, Brockmann *et al.* (37) reported that anti-inflammatory agent could play a pivotal role in

Fig. 11 Mean of relative cell viability (RCV) percentage depending on the tested material (**I**), tested concentrations (**II**), and cell line type (**III**). P value < 0.05 is considered significant.
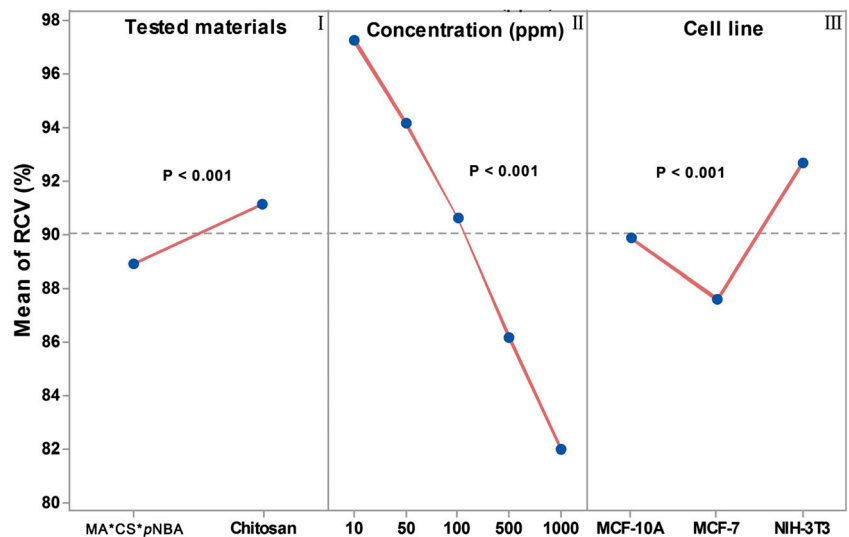
enhancing wound healing by preventing the infective pathogens to invasion into the blood of the damaged skin area via increasing the formation of collagen and fibroblast cells. Our findings of membrane stabilization were found consistent with our previous study (1), suggesting that the MA*CS*pNBA is a promising anti-inflammatory candidate valued for pharmaceutical applications. Anti-inflammatory properties of MA*CS*pNBA was also conducted by proteinase inhibitory activity. Various types of proteinases were released by lysosomic neutrophils, as a rich source of serine proteinase, to kill clinical pathogens as well as the development of damaged tissues during wound healing (1,38). The present study might be the first to explore the *in vitro* anti-inflammatory activity of MA*CS*pNBA Schiff base. Therefore, the current findings implicate that the MA*CS*pNBA has potential anti-inflammatory activity and

open windows for designing alternative antibacterial candidates effective in skin wound healing. Further *in vivo* study on Wistar albino rats infected with polymicrobial MDR pathogens is under investigation to clearly understand the exact mechanism of action of such newly modified chitosan derivative, especially after significant *in vitro* antibacterial, anti-biofilm, antioxidant and anti-inflammatory activities proved in this study.

In biomedical applications, hydrogel wound dressing, for example, is generally in contact with blood. Therefore, the hemolytic activity of any biomaterial that can promote skin wound healing must reach an acceptable range (39). It is necessary to take into account the hemocompatibility of MA*CS*pNBA, as a novel synthesized candidate, for its biological safety in pharmaceutical and biomedical formulations. In this context, the results of hemolytic activity are in

Fig. 12 Correlation between relative cell viability (RCV) percentage and concentration of tested material regardless of the type of material (**a**) or the type of cell line (**b**). *P* value < 0.05 is considered significant.
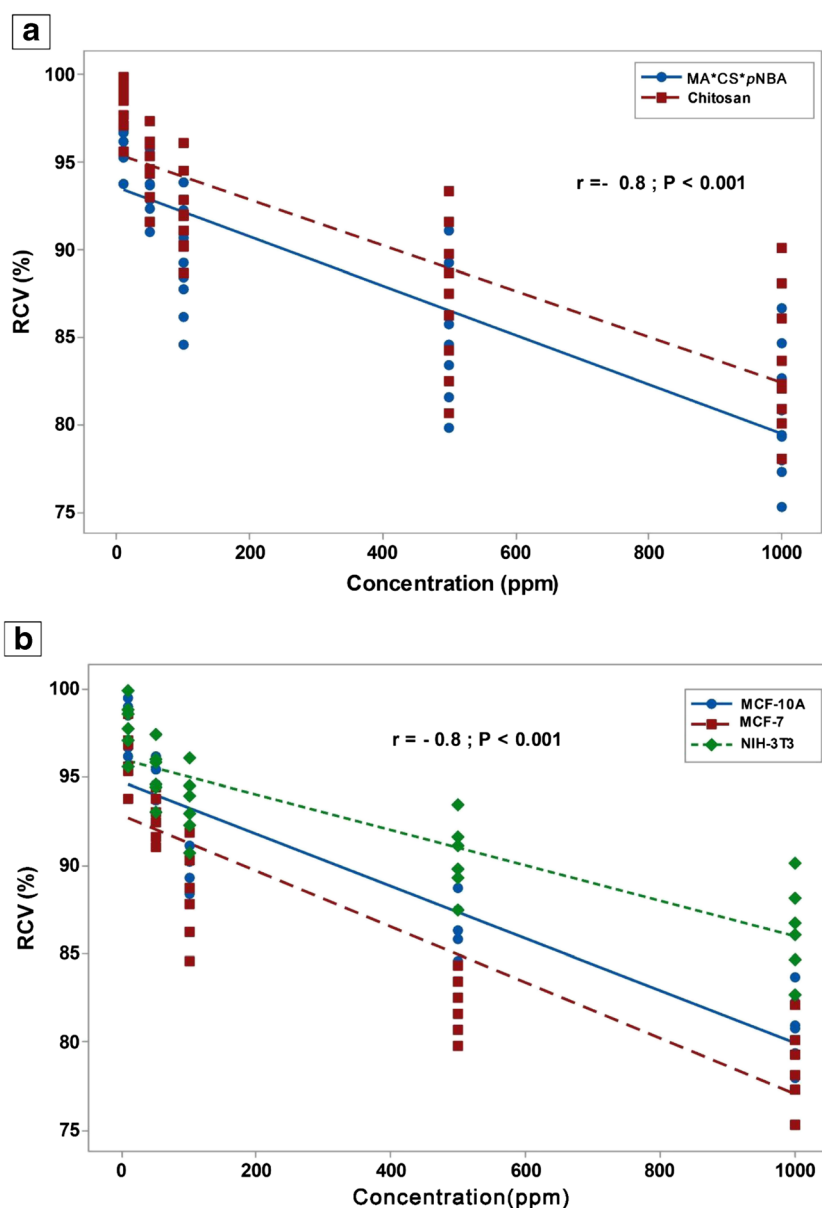
agreement with other studies in demonstrating that the chitosan derivatives do not cause hemolysis, do not affect the integrity of RBCs, and have excellent blood compatibility (19,39). Therefore, the hemocompatibility performance of MA*CS*pNBA might be promising to treat injured skin.

Cytotoxicity is also one of the most important detection assays to evaluate the biological safety of a material for biomedical and pharmaceutical applications. Biomedical material with RCV more than 70% was considered non-cytotoxic (22). The RCV exhibited a slight decline at the higher concentration of 1000 ppm, but still greater than 70% (22). We postulate that the reduction in the cytotoxicity of MA*CS*pNBA might be due to the rich amines in this modified polymer, which has good cell compatibility (40). Delocalization of positive charges onto the aromatic groups might be also one of the possible mechanisms (41,42). The excellent blood compatibility and no potential immunogenicity may be another mechanism that could reduce the cytotoxicity (22). Based on overall results, the novel chitosan derivative MA*CS*pNBA may have promising pharmaceutical activities, since in recent years pharmaceutical formulations have been extensively explored looking forward innovative possible treatments for several microbial infections, including skin burn wounds.

CONCLUSIONS

To the best of our knowledge, this study may be the first to investigate the pharmaceutical performance of a newly modified chitosan derivative, MA*CS*pNBA, obtained with a Schiff base reaction. Hemocompatibility and cytocompatibility results of this modified candidate exhibited to be promising for pharmaceutical application fields since it allied excellent and significant antibacterial activity against MDR bacterial pathogens, anti-biofilm, antioxidant, and anti-inflammatory activities. The efficiency of MA*CS*pNBA might be due to the presence of p-nitrobenzaldehyde conjugated with the aminated chitosan. Thus, this study may serve as a fruitful platform to explore chitosan derivatives as new leading structure valued for pharmaceutical and biomedical therapeutics with special reference to combating MDR bacteria of skin burn infections.

ACKNOWLEDGMENTS AND DISCLOSURES

REFERENCES

1. Ali SS, Morsy R, El-Zawawy NA, Fareed M, Bedaiwy MY. Synthesized zinc peroxide nanoparticles (ZnO2-NPs): a novel antimicrobial, anti-elastase, anti-keratinase, and anti-inflammatory approach toward polymicrobial burn wounds. Int J Nanomedicine. 2017;12:6059–73.

2. Ali SS, Shaaban MT, Abomohra A, El-Safity K. Macroalgal activity against multiple drug resistant *Aeromonas hydrophila*: a novel treatment study towards enhancement of fish growth performance. Microb Pathog. 2016;101:89–95.

3. Al-Tohamy R, Ali SS, Saad-Allah K, Fareed M, Ali A, El-Badry A, et al. Phytochemical analysis and assessment of antioxidant and antimicrobial activities of some medicinal plant species from Egyptian flora. J Appl Biomed. 2018;16:289–300.

4. El-Shouny WA, Ali SS, Sun JZ, Samy SM, Ali A. Drug resistance profile and molecular characterization of extended-spectrum beta-lactamase (ESβL)-producing *Pseudomonas aeruginosa* isolated from burn wound infections. Essential oils and their potential for utilization. Microb Pathog. 2018;116:301–12.

5. El Shafay SM, Ali SS, El-Sheekh MM. Antimicrobial activity of some seaweeds species from Red Sea, against multidrug resistant bacteria. Egypt J Aquat Res. 2016;42:65–74.

6. Grotz E, Tateosian N, Amiano N, Cagel M, Bernabeu E, Chiappetta DA, et al. Nanotechnology in tuberculosis: state of the art and the challenges ahead. Pharm Res. 2018;35:213.

7. Sarmento B, Ribeiro A, Veiga F, Sampaio P, Neufeld R, Ferreira D. Alginate/chitosan nanoparticles are effective for Oral insulin delivery. Pharm Res. 2007;24(12):2198–206.

8. Kusonwiriyawong C, Lipipun V, Vardhanabhuti N, Zhang Q, Ritthidej GC. Spray-dried chitosan microparticles for cellular delivery of an antigenic protein: Physico-chemical properties and cellular uptake by dendritic cells and macrophages. Pharm Res. 2013;30:1677–97.

9. Leung M, Forrest FM, Florczyk SJ, Veiseh O, Wu J, Park JO, et al. Chitosan-alginate scaffold culture system for hepatocellular carcinoma increases malignancy and drug resistance. Pharm Res. 2010;27:1939–48.

10. Liu Q, Zheng X, Zhang C, Shao X, Zhang X, Zhang Q, et al. Antigen-conjugated N-trimethylaminoethylmethacrylate chitosan nanoparticles induce strong immune responses after nasal administration. Pharm Res. 2015;32:22–36.

11. Grisin T, Bories C, Bombardi M, Loiseau PM, Rouffiac V, Solgadi A, et al. Supramolecular ChitosanMicro-platelets synergistically enhance anti-Candida albicans activity of amphotericin B using an immunocompetent murine model. Pharm Res. 2017;34:1067–82.

12. Morsy R, Ali SS, El-Shetehy M. Development of hydroxyapatite-chitosan gel sunscreen combating clinical multidrug-resistant bacteria. J Mol Struct. 2017;1143:251–8.

13. Mahmoudzadeh M, Fassihi A, Dorkoosh F, Heshmatnejad R, Mahnam K, Sabzyan H, et al. Elucidation of molecular mechanisms behind the self-assembly behavior of chitosan amphiphilic derivatives through experiment and molecular modeling. Pharm Res. 2015;32:3899–915.

14. Casettari L, Castagnino E, Stolnik S, Lewis A, Howdle SM, Illum L. Surface characterisation of bioadhesive PLGA/chitosan microparticles produced by supercritical fluid technology. Pharm Res. 2011;28:1668–82.

15. Tamer TM, Hassan MA, Omer AM, Baset WMA, Hassan ME, El-Shafeey ME, et al. Synthesis, characterization and antimicrobial evaluation of two aromatic chitosan Schiff base derivatives. Process Biochem. 2016;51:1721–30.

16. Malik S, Nema B. Antimicrobial activities of schiff bases: a review. Int J Theor Appl Phys. 2016;8:28–30.

17. Beg Ahmad AZ. Antimicrobial and phytochemical studies on 45 Indian medicinal plants against multi drug resistant human pathogens. J Ethnopharmacol. 2001;74:113–23.

18. Saranya TS, Rajan VK, Biswas R, Jayakumar R, Sathianarayanan S. Synthesis, characterization and biomedical applications of curcumin conjugated chitosan microspheres. Int J Biol Macromol. 2018;110:227–33.

19. Tan W, Zhang J, Zhao X, Dong F, Li Q, Guo Z. Synthesis and antioxidant action of chitosan derivatives with amino-containing groups via azide-alkyne click reaction and N-methylation. Carbohydr Polym. 2018;199:583–92.

20. Zhang J, Tan W, Wang G, Yin X, Li Q, Dong F, et al. Synthesis, characterization, and antioxidant activity of N,N,N,-trimethyl chitosan salts. Int J Biol Macromol. 2018;118:9–14.

21. Upadhyay J, Kumar A, Gogoi B, Buragohain AK. Antibacterial and hemolysis activity of polypyrrole nanotubes decorated with silver nanoparticles by an in-situ reduction process. Mater Sci Eng C. 2015;54:8–13.

22. Liu M, Min L, Zhu C, Rao Z, Liu L, Xu W, et al. Preparation, characterization and antioxidant activity of silk peptides grafted carboxymethyl chitosan. Int J Biol Macromol. 2017;104:732–8.

23. Regiel-Futyra A, JM D,b, Mazuryk O, S´ p K, Kyzioł A, Pucelik B, et al. Bioinorganic antimicrobial strategies in the resistance era. Coord Chem Rev. 2017;351:76–117.

24. Poonguzhali R, Basha SK, Kumari VS. Fabrication of asymmetric nanostarch reinforced chitosan/PVP membrane and its evaluation as an antibacterial patch for in vivo wound healing application. Int J Biol Macromol. 2018;114:204–13.

25. Sabaaa MW, Elzanaty AM, Abdel-Gawad OF, Arafa EG. Synthesis, characterization and antimicrobial activity of Schiff bases modified chitosan-graft-poly(acrylonitrile). Int J Biol Macromol. 2018;109:1280–91.

26. Anush SM, Vishalakshi B, Kalluraya B, Manju N. Synthesis of pyrazole-based Schiff bases of chitosan: evaluation of antimicrobial activity. Int J Biol Macromol. 2018;119:446–52.

27. Choi H, Kim KJ, Lee DG. Antifungal activity of the cationic antimicrobial polymer-polyhexamethylene guanidine hydrochloride and its mode of action. Fungal Biol. 2017;121:53–60.

28. Campana R, Biondo F, Mastrotto F, Baffone W, Casettari L. Chitosans as new tools against biofilms formation on the surface of silicone urinary catheters. Int J Biol Macromol. 2018;118:2193–200.

29. Perinelli DR, Fagioli L, Campana R, Lam JKW, Baffone W, Palmieri GF, et al. Chitosan-based nanosystems and their exploited antimicrobial activity. Eur J Pharm Sci. 2018;117:8–20.

30. Süntar I, Akkol EK, Nahar L, Sarker SD. Wound healing and antioxidant properties: do they coexist in plants? Free Radic Antioxid. 2012;2(2):1–7.

31. Soni B, Visavadiya NP, Madamwar D. Attenuation of diabetic complications by C- phycoerythrin in rats: antioxidant activity of C-phycoerythrin including copper induced lipoprotein and serum oxidation. Br J Nutr. 2009;102(1):102–9.

32. Divya K, Vijayan S, Jisha MS. Antifungal, antioxidant and cytotoxic activities of chitosan nanoparticles and its use as an edible coating on vegetables. Int J Biol Macromol. 2018;114:572–7.

33. Liu CH, Wang CH, Xu ZI, Wang Y. Isolation chemical characterization and antioxidant activities of two polysaccharides from the gel and the skin of aloe barbadensis, miller irrigated with sea water. Process Biochem. 2007;42:961–70.

34. Sadique J, Al-Rqodah WA, Baghhath MF, El-Ginay RR. The bioactivity of certain medicinal plants on the stabilization of the RBC system. Fitoterapia. 1989;66:525–32.

35. Anosike CA, Igboegwu ON, Nwodo OFC. Antioxidant properties and membrane stabilization effects of methanol extract of *Mucuna pruriens* leaves on normal and sickle erythrocytes. J Tradit Complement Med. 2018. https://doi.org/10.1016/j.jtcme.2017.08.002.

36. Govindappa M, Hemashekhar B, Arthikala MK, Rai VR, Ramachandra YL. Characterization, antibacterial, antioxidant, antidiabetic, anti-inflammatory and antityrosinase activity of green synthesized silver nanoparticles using *Calophyllum tomentosum* leaves extract. Results in Physics. 2018;9:400–8.

37. Brockmann L, Giannou AD, Gagliani N, Huber S. Regulation of TH17 cells and associated cytokines in wound healing, tissue regeneration, and carcinogenesis. Int J Mol Sci. 2017;18:1033.

38. Yadav E, Singh D, Yadav P, Verma A. Antioxidant and anti-inflammatory properties of *Prosopis cineraria* based phenolic rich ointment in wound healing. Biomed Pharmacother. 2018;108:1572–83.

39. Luo P, Nie M, Wen H, Xu W, Fan L, Cao Q. Preparation and characterization of carboxymethyl chitosan sulfate/oxidized konjac glucomannan hydrogels. Int J Biol Macromol. 2018;113:1024–31.

40. Mao S, Shuai X, Unger F, Wittmar M, Xie X, Kissel T. Synthesis, characterization and cytotoxicity of poly(ethylene glycol)-graft-trimethyl chitosan block copolymers. Biomaterials. 2005;26(32):6343–56.

41. Sajomsang W, Gonil P, Ruktanonchai UR, Petchsangsai M, Opanasopit P, Puttipipatkhachorn S. Effects of molecular weight and pyridinium moiety on water-soluble chitosan derivatives for mediated gene delivery. Carbohydr Polym. 2013;91(2):508–17.

42. Kenawy E, Ali SS, Al-Etewy M, Sun JZ, Wu J, El-Zawawy N. Synthesis, characterization and biomedical applications of a novel Schiff base on methyl acrylate-functionalized chitosan bearing *p*-nitrobenzaldehyde groups. Int J Biol Macromol. 2018. https://doi.org/10.1016/j.ijbiomac.2018.11.005.